

# High Salt Electrolyte Solutions Challenge the Electrochemical CO<sub>2</sub> Reduction Reaction to Formate at Indium and Tin Cathodes

Aykut Kas,<sup>[a]</sup> Paniz Izadi,<sup>[a]</sup> and Falk Harnisch<sup>\*[a]</sup>

Formate is a promising product of the electrochemical CO<sub>2</sub> reduction reaction (eCO<sub>2</sub>RR) that can serve as feedstock for biological syntheses. Indium (In) has been shown as a selective electrocatalyst of eCO<sub>2</sub>RR with high coulombic efficiency (CE) for formate production at small scale at biocompatible non-halophilic that is low salt conditions. Ohmic losses and challenges on potential/current distribution arise for scaling-up, where higher salt loads are advantageous for minimizing these. Higher salt concentration within the solution or halophilic conditions also enable the use of halophilic biocatalysts. We

optimized eCO<sub>2</sub>RR with halophilic media by introducing tin (Sn) as a more sustainable alternative to In. At 3% NaCl providing a catholyte conductivity ( $\kappa_S$ ) of 70 mS cm<sup>-1</sup>, the maximum specific formate production rates ( $r_{\text{formate}}$ ) of  $0.143 \pm 0.030$  mmol cm<sup>-2</sup> h<sup>-1</sup> and  $0.167 \pm 0.027$  mmol cm<sup>-2</sup> h<sup>-1</sup> were achieved at In and Sn electrocatalysts, respectively. Decrease in  $r_{\text{formate}}$  and CE, in addition to higher variation between replicates was observed with further increase in NaCl concentration above 3% ( $\kappa_S > 70$  mS cm<sup>-1</sup>) up to 10% ( $\kappa_S = 127$  mS cm<sup>-1</sup>). This study sets the foundation for integrated microbial synthesis by halophiles.

## Introduction

It is imperative to utilize CO<sub>2</sub> as feedstock to restrict global temperature increase and establish a circular economy. Various chemical, physical and biobased approaches are suggested to transform CO<sub>2</sub> into valuable fuels, chemicals, and building materials. Among these approaches is electrochemical CO<sub>2</sub> reduction reaction (eCO<sub>2</sub>RR) that uses electric energy to convert CO<sub>2</sub> into valuable compounds. Albeit formation of multi-carbon compounds requires the electrochemical formation of C–C bonds, the majority of studies reported the formation of C<sub>1</sub>-compounds such as carbon monoxide (CO), formate/formic acid (HCOO<sup>-</sup>/HCOOH), formaldehyde (CH<sub>2</sub>O) and methane (CH<sub>4</sub>). Formate is a valuable building block for chemical processes,<sup>[1]</sup> can serve as feedstock for microbial synthesis<sup>[2–5]</sup> and is a promising intermediate for storage of (electric) energy.<sup>[6]</sup> For achieving eCO<sub>2</sub>RR to formate Eq. (1), metal electrocatalysts at cathodes including lead, mercury, bismuth, cadmium, copper, indium and tin are typically used.<sup>[7,8]</sup> Tin (Sn) and indium (In) based electrocatalysts possess a high selectivity for eCO<sub>2</sub>RR to formate rather than hydrogen evolution reaction (HER, [Eq. (2)]).<sup>[9,10]</sup> We kindly refer the readers to reviews for comprehensive molecular understanding of In and Sn catalysts,

their morphology and surface structures that is not in focus for this study.<sup>[9,11]</sup> Previously, highly selective and efficient eCO<sub>2</sub>RR to formate under biocompatible mesophilic conditions (i.e., ambient  $T$ ,  $p$  and neutral pH) at In was demonstrated.<sup>[12–14]</sup> Formate production rate ( $r_{\text{formate}}$ ) and coulombic efficiency (CE) in this setup (see also Figure 1) at the cathodic potential of  $-1.6$  V vs. Ag/AgCl, were  $0.013 \pm 0.002$  mmol cm<sup>-2</sup> h<sup>-1</sup> and  $64.6 \pm 6.8\%$ , respectively.<sup>[14]</sup> In a subsequent study using the similar setup and catholyte (50 mM HCO<sub>3</sub> buffer), higher  $r_{\text{formate}}$  and CE were achieved when the cathodic potential of  $-2.2$  V vs. Ag/AgCl was applied, reaching the  $r_{\text{formate}}$  of  $0.061 \pm 0.007$  mmol cm<sup>-2</sup> h<sup>-1</sup> and CE of  $93.0 \pm 2.4\%$ .<sup>[13]</sup> Despite this

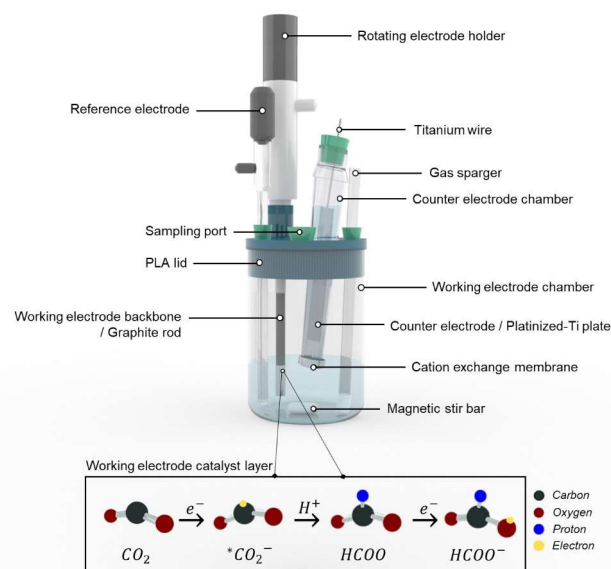


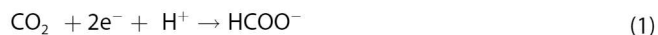
Figure 1. Electrochemical reactor and setup used throughout the eCO<sub>2</sub>RR experiments (details see text).

[a] A. Kas, Dr. P. Izadi, Prof. Dr. F. Harnisch  
Department of Environmental Microbiology,  
Helmholtz-Centre for Environmental Research – UFZ,  
Leipzig, Germany  
E-mail: falk.harnisch@ufz.de

Supporting information for this article is available on the WWW under <https://doi.org/10.1002/celec.202300311>

© 2023 The Authors. ChemElectroChem published by Wiley-VCH GmbH. This is an open access article under the terms of the Creative Commons Attribution License, which permits use, distribution and reproduction in any medium, provided the original work is properly cited.

excellent performance using In is no option at technical scale, as In is considered to have a high supply risk and is hence included in the EU's list of Critical Raw Materials (CRMs) since 2010.<sup>[15]</sup>



As opposed to In, Sn is accessible, cheap and has also been widely used in eCO<sub>2</sub>RR studies, displaying high selectivity for formate production with high CE. Sn is occasionally combined with other metals, such as Cu-Sn<sup>[16]</sup> and Pd/Sn alloy on activated carbon<sup>[17]</sup> to enhance performance, achieving near 100% CE with KHCO<sub>3</sub> buffers. Studies using only Sn as eCO<sub>2</sub>RR electrocatalyst achieved CEs with pure Sn rods at -1.6 V vs. Ag/AgCl at 94%,<sup>[18]</sup> Sn on graphene at -1.76 V vs. Ag/AgCl reaching 89%,<sup>[19]</sup> and Sn on carbon nanofibers at -1.42 V vs. Ag/AgCl with 62% CE.<sup>[20]</sup>

Limitation of the product spectrum of the eCO<sub>2</sub>RR to mainly C<sub>1</sub>-compounds initiated the development of concepts that interface the eCO<sub>2</sub>RR to a subsequent microbial synthesis, as these may lead to diversity of high-value products.<sup>[6,21–23]</sup> An exemplary demonstration of this concept for eCO<sub>2</sub>RR to CO (and H<sub>2</sub>) that are used for subsequent gas fermentation achieved almost 100% CE for production of alcohols.<sup>[24]</sup> Combining eCO<sub>2</sub>RR with microbial catalysis for formate utilization allowed production of mesaconate and 2S-methylsuccinate by *Methylobacterium extorquens* AM-1,<sup>[25]</sup> alcohols and polyhydroxybutyrate (PHB) by *Cupriavidus necator*<sup>[26]</sup> and amino acids by synthetically modified *Escherichia coli*.<sup>[27]</sup>

Extremophiles are microorganisms that adapted to thrive in extreme conditions in their natural habitats such as low and high temperature (cryophiles and thermophiles) or high salt concentration (halophiles). Halophiles are of particular interest to be exploited by interfacing to electrochemical reactions, as highly saline conditions allow high concentrations of the supporting electrolyte that is leading to lower energetic losses.<sup>[28]</sup> Additionally, halophiles are utilized in biotechnological

processes to produce specific high-value bioproducts<sup>[29,30]</sup> by synthesizing compatible solutes (e.g., ectoine, hydroxyectoine, proline) to counteract osmotic stress. Exploiting them in microbial electrosynthesis could provide a new avenue to target high-value products from waste streams, in this case starting from CO<sub>2</sub>.

Interfacing the eCO<sub>2</sub>RR to formate with microbial synthesis from formate, especially in situ that is in one vessel, requires developing an electrolyte composition being optimal for both microbial growth and abiotic electrosynthesis. Therefore, the optimal electrolytic conductivity ( $\kappa_s$ ) and salt concentration favoring both microbial and electrochemical processes were investigated. This is specifically important due to the decrease in internal resistance and the required power output at higher  $\kappa_s$ , but decrease in saturation concentration of CO<sub>2</sub>.<sup>[31]</sup> To investigate the effect of halophilic growth media components (buffer, mineral salt, and NaCl concentrations) on eCO<sub>2</sub>RR to formate, the previously established reactor setup was used<sup>[12–14,32]</sup> starting from the model medium for halophiles MM63.<sup>[33]</sup> Sn and In for eCO<sub>2</sub>RR were compared for formate production rates, CE, and electrocatalyst leaching. In particular, NaCl was investigated in this study as it is an essential compound for the growth and activity of halophilic microorganisms.<sup>[34–36]</sup>

## Results and Discussion

### Establishment of Sn-electrodeposition on graphite electrodes

Figure 2 shows the eCO<sub>2</sub>RR to formate at In cathodes at -2.2 V under identical experimental conditions as the previous study.<sup>[13]</sup> Reproducible performance was observed, reaching the production rate of  $r_{\text{formate}} = 0.086 \pm 0.003 \text{ mmol cm}^{-2} \text{ h}^{-1}$  and even slightly higher coulombic efficiency (CE = 92.1 ± 0.4%). In order to allow linkage to earlier work, we performed tests on Sn at -1.6 V and -2.2 V, utilizing well-established methodology used for studying In.<sup>[12–14,32]</sup> In-catalyst setup was first established at -1.6 V<sup>[14]</sup> and later optimized at -2.2 V among a range

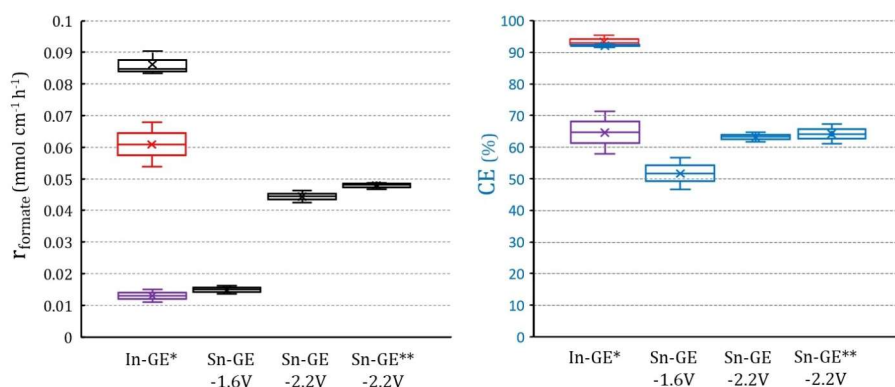


**Figure 2.** Specific formate production rate ( $r_{\text{formate}}$ ) and coulombic efficiency (CE) of established In-catalyst setup (In-GE) and results with new Sn-catalyst at the graphite electrode (Sn-GE). During the eCO<sub>2</sub>RR experiments, 50 mM NaHCO<sub>3</sub> electrolyte solution was used at the applied potentials ( $E_{\text{prod}}$  vs. Ag/AgCl, in satd. KCl) indicated below the bar graphs ( $n=3$ ). \* Benchmark results from our previous study using In-catalysts in the identical setup are shown in purple box plot (at  $E_{\text{prod}} = -1.6 \text{ V}$ ),<sup>[14]</sup> red box plot (at  $E_{\text{prod}} = -2.2 \text{ V}$ )<sup>[13]</sup> and this study in black/blue box plots (at  $E_{\text{prod}} = -2.2 \text{ V}$ ). \*\* Electrodeposition charge ( $Q_{\text{ed}}$ ) increased from 1 C to 3 C.

of potentials between  $-1.6$  to  $-3.0$  V.<sup>[13]</sup> Further, investigation on operating 72 h at different potentials ranging from  $-1.6$  to  $-2.2$  V showed that at  $-2.2$  V highest formate concentration were achieved.<sup>[32]</sup> Therefore, for evaluating the performance of the Sn cathodes, the two exemplary potentials  $-1.6$  V and  $-2.2$  V were selected. When  $-1.6$  V was applied at the Sn-cathodes,  $r_{\text{formate}}$  and CE reached to  $0.015 \pm 0.001$  mmol cm<sup>-2</sup> h<sup>-1</sup> and  $51.7 \pm 7.1$  %, respectively (Figure 2). Although CE increased only to  $63.2 \pm 2.1$  % at an applied potential of  $-2.2$  V during experiments,  $r_{\text{formate}}$  improved notably to  $0.046 \pm 0.004$  mmol cm<sup>-2</sup> h<sup>-1</sup>. With Sn cathodes,  $r_{\text{formate}}$  and CE values were lower than these using In cathodes in 50 mM KHCO<sub>3</sub> at the same potentials, but they were still comparable with Sn-coated carbon paper electrodes that showed approximately 63 % CE at  $E_{\text{prod}} = -2.0$  V in 100 mM KHCO<sub>3</sub> electrolyte.<sup>[37]</sup>

As the  $r_{\text{formate}}$  values achieved using Sn was not comparable with those at In electrodes, further tests were performed to improve the electrodeposition method. The impact of increasing the electrodeposition charge, which led to a thicker catalyst layer (theoretically calculated to be  $3.375$  μm for  $Q_{\text{ed}} = 3$  C, Figure S1) was investigated. However, this resulted in only a slight increase in formate production and no change in CE. Therefore, electrodeposition potential of  $-1.0$  V and 3 C charge were selected (described in Supplementary Information) for all follow-up investigations as it yielded the highest formate production rate of  $0.048 \pm 0.001$  mmol cm<sup>-2</sup> h<sup>-1</sup> at a CE of  $64.2 \pm 3.2$  % in 50 mM NaHCO<sub>3</sub> that served as a benchmark.

A reliable and reproducible electrodeposition method for Sn on graphite electrodes was established for the eCO<sub>2</sub>RR. As it was previously established with the In electrocatalyst setup

before and replicated here, results obtained in this part with Sn serve as a benchmark for the stable operation as well as performance of eCO<sub>2</sub>RR to formate. Further optimization of the Sn-catalyst setup for scaling up or long-term operation may be of interest, as production rates certainly might be improved, e.g. by pulsed potential operational mode.<sup>[37,38]</sup>

### Increasing NaCl concentration of halophilic media enhances electrochemical formate production at the cost of lower selectivity

As an initial step towards integrating eCO<sub>2</sub>RR to formate at high salinity and its interfacing with halophilic microbial catalysis using formate, the effect of MM63 V media composition on the electrochemical processes was studied. The MM63 V medium is thereby representative of a model halophilic growth medium, as it is used for various pure culture halophilic strains.<sup>[39–43]</sup>

In the previous work with the same reactor setup, CE and  $r_{\text{formate}}$  of ca. 85 % and  $0.2$  mmol cm<sup>-2</sup> h<sup>-1</sup> were achieved at the In-cathodes using 50 mM NaHCO<sub>3</sub> with the conductivity adjusted at  $20$  mS cm<sup>-1</sup> using Na<sub>2</sub>SO<sub>4</sub>.<sup>[13]</sup> When MM63 V medium (without NaCl) with a similar conductivity as the carbonate buffer ( $\kappa_S = 17.9$  mS cm<sup>-1</sup>) was used, CE decreased to  $34.0 \pm 2.0$  % for In,  $41.4 \pm 3.2$  % for Sn, although  $r_{\text{formate}}$  increased to  $0.106 \pm 0.003$  mmol cm<sup>-2</sup> h<sup>-1</sup> for In and  $0.126 \pm 0.006$  mmol cm<sup>-2</sup> h<sup>-1</sup> for Sn (Figure 3). With 3 % NaCl added to MM63 V ( $\kappa_S = 70$  mS cm<sup>-1</sup>),  $r_{\text{formate}}$  increased to  $0.143 \pm 0.032$  mmol cm<sup>-2</sup> h<sup>-1</sup> and  $0.167 \pm 0.027$  mmol cm<sup>-2</sup> h<sup>-1</sup> at In and Sn electrocatalysts, respectively. Despite the increase in  $r_{\text{formate}}$

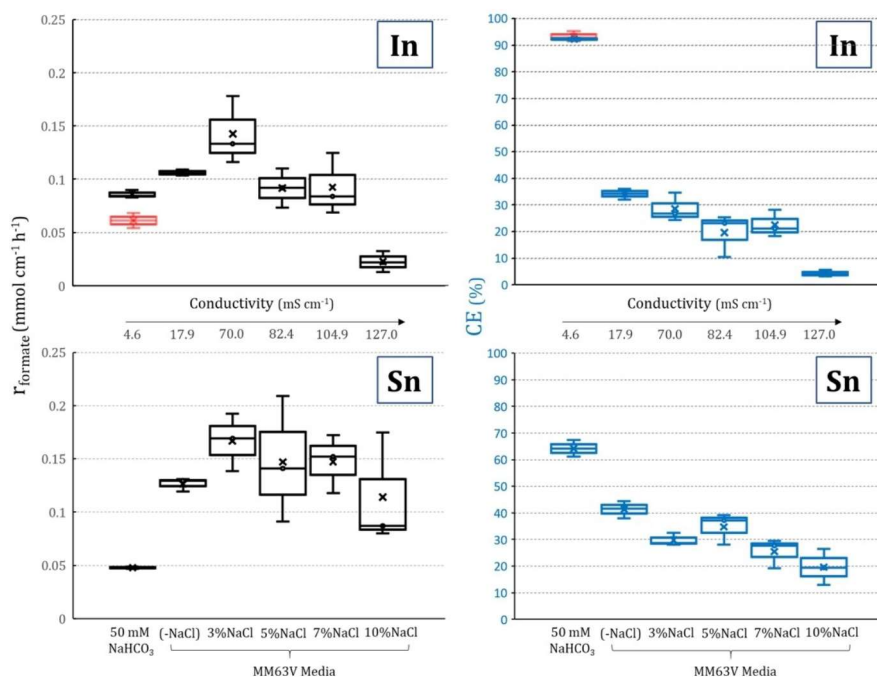


**Figure 3.** Specific formate production rate ( $r_{\text{formate}}$ ) and coulombic efficiencies (CE) achieved during eCO<sub>2</sub>RR at In-coated graphite electrode and Sn-coated graphite electrode with modified minimal media (MM63 V). A potential of  $-2.2$  V vs. Ag/AgCl in sat. KCl was applied at the electrodes for  $t = 1$  h at  $T = 30$  °C ( $n = 3$ ).  $\kappa_S$ , initial and final pH of the different growth medium experiments are summarized in Table S2. Box plots in red shows the results from<sup>[13]</sup> using the identical setup and conditions.

CEs declined to  $28.4 \pm 5.4\%$  for In and  $41.4 \pm 3.2\%$  for Sn. This increase in the  $r_{\text{formate}}$  was notable, but most likely not specific to the NaCl addition. For instance the 3% NaCl MM63 V ( $\kappa_5 = 70 \text{ mS cm}^{-1}$ ) did not reach the  $r_{\text{formate}}$  when conductivity-adjusted bicarbonate buffer using  $\text{Na}_2\text{SO}_4$  ( $\kappa_5 = 20 \text{ mS cm}^{-1}$ ,<sup>[13]</sup> and  $\kappa_5 = 21 \text{ mS cm}^{-1}$ <sup>[32]</sup>) was used at a lower  $\kappa_5$  value from previous studies for 1 hour of  $\text{eCO}_2\text{RR}$ . Increasing conductivity from  $4.5 \text{ mS cm}^{-1}$  to  $10 \text{ mS cm}^{-1}$  using  $\text{NaSO}_4$  led to increase in  $r_{\text{formate}}$  of up to two times with In electrodes, reaching  $0.136 \pm 0.016 \text{ mmol cm}^{-2} \text{ h}^{-1}$ , while two fold increase was also observed simultaneously in the cathodic current.<sup>[13]</sup> This could be justified by higher HER rather than  $\text{eCO}_2\text{RR}$ , which in turn decreased the CE value. This aligns with,<sup>[44]</sup> which stated that the current density for CO or  $\text{HCO}_3^-$  formation could be limited given low  $\text{CO}_2$  solubility in water at ambient conditions. Considering our case, although constant supply of  $\text{CO}_2$  before and throughout the experiment enabled formate production to continue, it was likely that higher conductivity leading to higher current fostered HER, due to depletion of  $\text{CO}_2$  at the cathode surface. This phenomenon might be attributed to the reaction being limited by mass transfer, and insufficient  $\text{CO}_2$  or  $\text{HCO}_3^-$  diffusion to the electrocatalyst active sites, while  $\text{H}^+$  could easily move to the cathode surface due to Grothuss mechanism-based transport,<sup>[45]</sup> thus becoming readily available as reactant, for instance, for HER. This could be overcome by optimizing the reactor configuration and electrode architecture, e.g., using a gas diffusion electrode (GDE) design, in which the mass transfer limitations can be tackled.<sup>[46]</sup> Additionally, it was previously shown<sup>[47]</sup> that the influence of  $\text{KHCO}_3$  concentration on  $\text{eCO}_2\text{RR}$  could be due to the  $\text{K}^+$  ions blocking the electrode surface and consequently preventing the cathodic reaction with non-polar  $\text{CO}_2$  reactants. The larger Stokes radius of hydrated  $\text{Na}^+$  (1.94 Å) compared to  $\text{K}^+$  (1.34 Å) was suggested to intensify this surface blocking effect.<sup>[48]</sup>

Although acidic pH conditions at the cathode were previously reported to suppress  $\text{eCO}_2\text{RR}$  and favor HER,<sup>[49]</sup> this seems unlikely in our experiments, as minimal pH changes were observed during the one-hour operation (Table S2). After 1 hour of  $\text{eCO}_2\text{RR}$  with various halophilic media, pH increased only slightly (change was below 0.7 pH-units for all experiments). All initial pH values of the electrolyte solution/growth media, pH after reaching  $\text{CO}_2$  saturation (also shown in Figure S3) with approximately 10 min of sparging before experiment and at the end of 1 h experiment are summarized in Table S2. In addition, elevated HER rates more likely caused a detrimental  $\text{H}_2$  gas bubble formation that may prevent the availability of  $\text{CO}_2$  or  $\text{HCO}_3^-$  on the cathode surface, consequently making HER more dominant reaction than  $\text{eCO}_2\text{RR}$ . Higher gas production at the cathode was visually observed both in this study and previously<sup>[13]</sup> where higher  $\kappa_5$  yielding higher cathodic currents.

Increasing salt concentration beyond 3% NaCl (corresponding to  $70 \text{ mS cm}^{-1}$ ) led to a decline in both  $r_{\text{formate}}$  and CE, suggesting a further shift of electrons toward competing side reactions (Figure 3). This adverse effect was more pronounced for In, as  $r_{\text{formate}}$  decreased below benchmarking conditions using 50 mM bicarbonate buffer electrolyte solution when NaCl concentration exceeded 5%. The  $r_{\text{formate}}$  were approximately 1.6

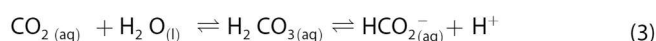
times higher at Sn-cathodes than at In-cathodes using both 5% and 7% NaCl halophilic media. Ultimately, at the highest NaCl concentration (10%,  $127 \text{ mS cm}^{-1}$ ),  $r_{\text{formate}}$  reached its lowest value ( $0.023 \pm 0.010 \text{ mmol cm}^{-2} \text{ h}^{-1}$ ), with CE dropping to  $4.1 \pm 1.2\%$  at In-cathodes. Meanwhile, relatively high  $r_{\text{formate}}$  of  $0.114 \pm 0.053 \text{ mmol cm}^{-2} \text{ h}^{-1}$  was achieved at Sn-cathodes. Although not as thoroughly optimized as the In-cathodes, the Sn-cathodes configuration demonstrated better performance of the  $\text{eCO}_2\text{RR}$  with NaCl concentrations above 3% using MM63 V media.

Several factors may have contributed decrease in CE, such as operational issues (described in SI. 2.2) associated with halophilic media as selectivity shifts towards side reactions, and electrocatalyst loss or inactivation through blocking of cathode surface with  $\text{Na}^+$  ions. Cations are known to interact non-covalently with  $\text{CO}_2$  and  $\text{eCO}_2\text{RR}$  intermediates on the cathode surface through electrostatic interactions or affect the local pH at the electrochemical interface and thus change the proton-coupled electron transfer (PCET).<sup>[50]</sup> The observed effects may potentially be also relevant for the concentration of cations present in the halophilic media. Yet, this molecular level investigation was not in focus for our current study. For achieving a high selectivity of  $\text{eCO}_2\text{RR}$ , ions in the electrolyte solution, distinct from those involved in the targeted reaction, must remain electrochemically inert without undergoing oxidation or reduction under the applied conditions. Water is the primary proton source in  $\text{eCO}_2\text{RR}$ , but buffering anions with lower pKa values might also serve as proton donors and enhance the reaction rates.<sup>[7]</sup> Additionally, adsorption of halides on the electrode surface was reported to influence charge density and selectivity surface structure and morphology during oxidation-reduction cycles.<sup>[51]</sup> In accordance with our previous findings regarding the long-term operation of the In-catalyst, the HER rates seemed to increase over time, and electrons were majorly utilized in HER rather than  $\text{eCO}_2\text{RR}$ .<sup>[32]</sup> The  $\text{eCO}_2\text{RR}$  is highly dependent on the applied potential, with the first electron transfer to  $\text{CO}_2$  molecules being described as the rate-limiting step.<sup>[45]</sup> Previous studies with In-catalyst have shown a significant increase in both CE and  $r_{\text{formate}}$  at  $-2.2 \text{ V}$  compared to  $-1.6 \text{ V}$ .<sup>[13,32]</sup> Even at higher overpotentials, the surprisingly high selectivity was maintained at In-catalyst with CE being  $86.8 \pm 16.1\%$  at  $-3.0 \text{ V}$ , while already at  $-2.2 \text{ V}$  a CE of  $93.0 \pm 2.4\%$  was reached.<sup>[13]</sup> Throughout the 72 h experiments in the previous study at  $-2.2 \text{ V}$  applied potential,<sup>[32]</sup> the changes in the overpotentials of  $\text{eCO}_2\text{RR}$  or HER were negligible and unlikely to influence the selectivity shift at any stage of the experiment. Selectivity shift was more likely due to electrocatalyst unavailability or based on other mechanistic factors related to  $\text{CO}_2$  availability rather than a thermodynamic advantage as also previously described.<sup>[13,32]</sup> Since the electrochemical cell used in our study was not designed fully gas-tight, a complete quantification of gaseous products was not conducted. Only hydrogen gas using gas chromatography and formate were observed with HPLC measurements. Although it was not desired in this study, HER could be advantageous for future integrated system. For instance,  $\text{H}_2$  could be a source of energy in addition to formate for some microbes or synthetic

engineered strains, when microbial processes for biosynthesis and eCO<sub>2</sub>RR are combined.<sup>[52,53]</sup>

### $\kappa_5$ increase affects eCO<sub>2</sub>RR rate rather than buffer type or concentration

As shown in Eq. (3), CO<sub>2</sub> dissolving in aqueous solutions forms an equilibrium with carbonic acid (H<sub>2</sub>CO<sub>3</sub>), which dissociates into bicarbonate ions (HCO<sub>3</sub><sup>-</sup>) and protons (H<sup>+</sup>). Bicarbonate ion plays a unique role in eCO<sub>2</sub>RR by enhancing CO<sub>2</sub> solubility, facilitating proton-coupled electron transfer, and acting as a reactant or intermediate.<sup>[31]</sup> Despite the decrease in CO<sub>2</sub> solubility at higher salt concentrations, the catholytes were saturated with CO<sub>2</sub> gas (Figure S3) after approximately 10 minutes.



As shown above, using MM63 V medium (without NaCl) instead of 50 mM NaHCO<sub>3</sub> as catholytes led to decrease in eCO<sub>2</sub>RR performance. Thus, the lower bicarbonate concentration seems a likely explanation for the 60% decrease in CE observed when using MM63 V media with phosphate buffer (Figure 3 and Figure 4). To determine, if the absence of bicarbonate in MM63 V medium was responsible for this variation, two further sets of experiments were performed using either a lower (50 mM HCO<sub>3</sub><sup>-</sup>) or higher concentration (500 mM

HCO<sub>3</sub><sup>-</sup>) instead of 100 mM phosphate buffer with MM63 V (without NaCl).

Using In-cathodes, the addition of mineral salts (excluding NaCl) to the MM63 V medium or an increase in  $\kappa_5$  (from 4.5 to 6.4 mS cm<sup>-1</sup>, a 50% increase) led to a noteworthy decrease by around 40% in both  $r_{\text{formate}}$  to 0.052 ± 0.008 mmol cm<sup>-2</sup> h<sup>-1</sup> and CE to 54.2 ± 9.0% (Figure 4). An increase in the bicarbonate buffer concentration to 500 mM led to higher  $r_{\text{formate}}$  of 0.130 ± 0.033 mmol cm<sup>-2</sup> h<sup>-1</sup>, where both the enhanced buffering capacity and  $\kappa_5$  (34.0 mS cm<sup>-1</sup>) may have played a role, as also discussed previously.<sup>[13]</sup> The CE achieved using 500 mM HCO<sub>3</sub><sup>-</sup> (35.1 ± 3.7% at In, 51.1 ± 8.0% at Sn) was similar to that when 100 mM phosphate buffer was used as a supporting electrolyte (34.0 ± 2.0% at In, 41.4 ± 3.2% at Sn). This suggests that the presence of bicarbonate alone does not increase the selectivity of  $r_{\text{formate}}$ , but also leads to decrease in CEs. Using the same reactor setup as this study, it was shown that increasing HCO<sub>3</sub><sup>-</sup> concentration to 500 mM from 50 mM by keeping  $\kappa_5$  constant did not change formate production rates but decreased CE.<sup>[13]</sup> Presence of bicarbonate was shown to enhance the rate of eCO<sub>2</sub>RR to CO at gold electrodes by increasing the effective CO<sub>2</sub> concentration near electrode surface.<sup>[54]</sup> In our case, initial HCO<sub>3</sub><sup>-</sup> concentration in halophilic media as a sole parameter for improving eCO<sub>2</sub>RR to formate did not have a high impact on the overall performance, as CE and  $r_{\text{formate}}$  values remained almost stable. This was noteworthy considering the fact that MM63 V medium with 500 mM bicarbonate buffer had almost double  $\kappa_5$  and a high concentration of HCO<sub>3</sub><sup>-</sup> compared to 100 mM phosphate buffer with MM63 V. For explaining the

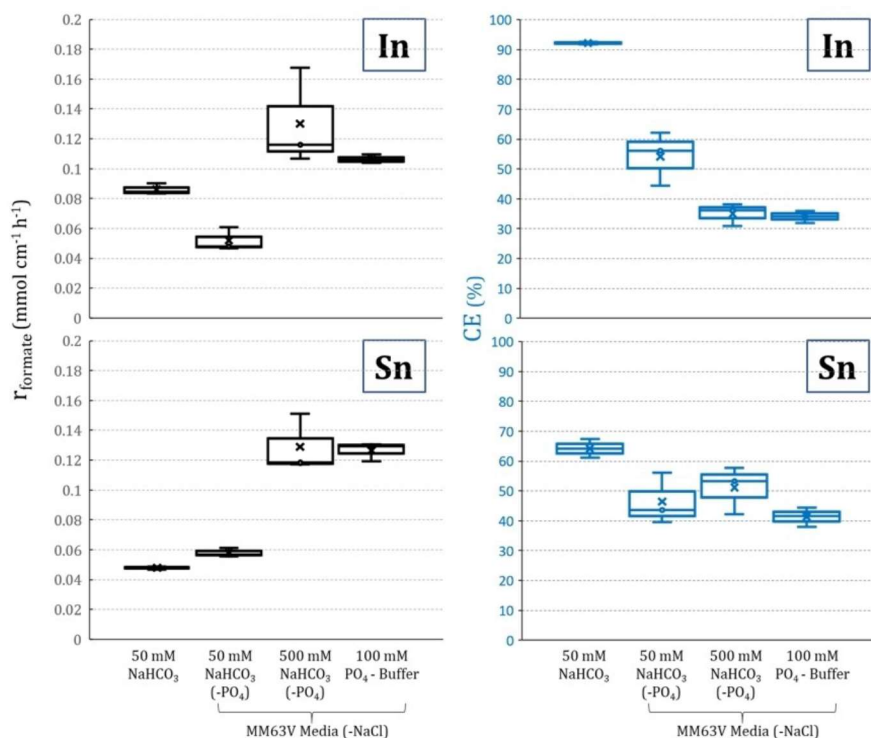


**Figure 4.** The effect of buffer concentration and type in MM63 V medium and 50 mM NaHCO<sub>3</sub> electrolyte solutions on eCO<sub>2</sub>RR performance at In-coated and Sn-coated graphite electrodes. The potential of -2.2 V vs. Ag/AgCl in saturated KCl was applied for  $t = 1$  h at  $T = 30$  °C ( $n = 3$ ).  $\kappa_5$ , initial and final pH of the different growth medium experiments are summarized in Table S2.

decrease in CE, it was previously suggested that  $\text{HCO}_3^-$  serves as a reactant for the HER as well.<sup>[55,56]</sup>

Similar to the high salt medium experiment with Sn,  $r_{\text{formate}}$  was enhanced at In-cathodes to the respective value of  $0.058 \pm 0.003 \text{ mmol cm}^{-2} \text{ h}^{-1}$  and  $0.129 \pm 0.019 \text{ mmol cm}^{-2} \text{ h}^{-1}$  using 50 mM and 500 mM  $\text{HCO}_3^-$  MM63 V media. This improvement seemed to be attributed to the increased  $\kappa_5$  rather than the buffering capacity or the initial availability of dissolved  $\text{CO}_2$  species when considering the similar results obtained when using 100 mM phosphate buffer and 500 mM  $\text{HCO}_3^-$ .

### Catalyst loss increased with the halophilic media as electrolyte solutions

When 50 mM  $\text{NaHCO}_3$  buffer or 7% NaCl MM63 V medium was provided, no formate production was monitored at the bare graphite. All charge was spent on HER, as expected for a carbon-based electrode with the applied potential more negative than  $-0.8 \text{ V}$ .<sup>[57]</sup> Therefore, it was hypothesized that selectivity shift towards HER from  $\text{eCO}_2\text{RR}$  to formate at the In as well as Sn cathodes could be due to electrocatalyst loss from the graphite electrode surface. At the end of the experiments conducted under high salinity conditions ( $\geq 3\%$  NaCl) for 1 h, the uniform electrocatalyst coating on the graphite surface (Figure S1) visually seemed to be no longer present, confirming the potential electrocatalyst loss. Therefore, potential electrocatalyst leaching to the catholyte was determined with polarography (Figure 5). The electrocatalyst loss increased almost 4 times for Sn and 8 times for In for halophilic medium (10% NaCl) in comparison to when 50 mM  $\text{HCO}_3^-$  buffer was used. Overall, it did not exceed 6% in any case (Figure 5) and therefore cannot solely account for the major selectivity shift.

Contribution of the electrocatalyst loss to any selectivity shift effect was previously described as negligible,<sup>[13,14,25]</sup> where it was found to be less than 1%. However, electrocatalyst leaching seemed to be more problematic with the use of halophilic media during this study as well as during extended

periods of operation up to 72 h with the identical electrochemical setup using In-catalyst.<sup>[32]</sup> Further research is required to study the electrocatalyst leaching and/or activating the catalyst during the  $\text{eCO}_2\text{RR}$ , e.g., by pulsing techniques. For instance, it was reported before that alkali metal ions can cover the electrocatalyst layer, leading to its inactivation.<sup>[47]</sup> Additionally, changes in the electrocatalyst layer and graphite backbone's surface chemistry due to inert by-product deposition, as previously reported,<sup>[11]</sup> should be considered.

### Conclusions and Outlook

In this study, we showed that it is possible to balance enhancing the performance of the abiotic  $\text{eCO}_2\text{RR}$  to formate with using halophilic media for microbial synthesis, while maintaining stability for scalability and reproducibility. To replace In with a more sustainable alternative, we introduced and systematically assessed Sn for  $\text{eCO}_2\text{RR}$  using halophilic MM63 V media with NaCl concentration varying between 0 to 10%. The performance of  $\text{eCO}_2\text{RR}$  to formate was maximized at both In and Sn electrocatalysts at 3% NaCl, with rates being increased 66% using In and 247% using Sn as electrocatalysts compared to simple buffer electrolytes (50 mM  $\text{HCO}_3^-$ ). It was likely that excess current yielding from the increased  $\kappa_5$  contributed to increased hydrogen production, which in turn adversely affected the stability of the electrocatalyst and the CE of  $\text{eCO}_2\text{RR}$ . Compared to simple buffer electrolytes, addition of mineral salts and increasing NaCl concentration caused a selectivity shift to competing side reactions that affected In-cathode more unfavorably for formate production compared to Sn-cathode. Compounds in the halophilic media including NaCl and other mineral salts have been observed to adversely affect the CE of  $\text{eCO}_2\text{RR}$  to formate. Further investigation on the effects of individual cations or anions while using electrolytes other than simple buffer systems could yield important information regarding its impact on the mechanisms and hence CE. Nonetheless, overall rates of formate production through electrochemical process was also improved with the increased conductivity of the electrolyte. Impact on CE is not the most crucial factor in establishing high salt electrosynthesis since other byproducts, such as hydrogen, can also be utilized by certain microorganisms. But eventually, conducting a detailed consideration of CE for the economic feasibility of the overall process is still required. Since progress has been made in improving formate production with a model growth medium for halophiles, next step is their integration with  $\text{eCO}_2\text{RR}$  at these high salt environments and utilizing electrochemically generated formate for biosynthesis of valuable end products, which is under investigation.

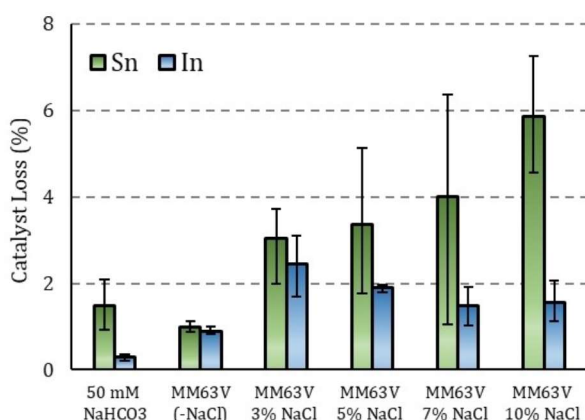


**Figure 5.** Measurement of electrocatalyst leaching to catholyte with polarography for Sn and In. Electrocatalyst loss (%) is calculated from the theoretical mass of electrocatalyst on graphite electrode surface based on the charge applied during electrodeposition (1.7 C for In and 3 C for Sn).

## Experimental Section

### General remarks

All potentials are reported versus Ag/AgCl sat. KCl [0.197 V vs. standard hydrogen electrode (SHE)]. All compounds were at least of an analytical grade. The polarography standards were made in tri-distilled water, all other solutions were prepared with de-ionized water (Merck Millipore, Germany). All modified halophilic media were autoclaved before use. All eCO<sub>2</sub>RR experiments were conducted in triplicate, and the data are presented as the mean value with their corresponding standard deviation.

### Electrochemical reactor setup and operation

An established<sup>[12–14]</sup> two-chamber electrochemical cell with an in-house produced glass counter electrode chamber and 3-D printed lid was used throughout eCO<sub>2</sub>RR experiments. Working electrode (cathode) chamber was a 400 mL glass beaker with an active volume of 50 mL. The anode (counter electrode), was placed in a glass tube and was in contact with the cathode chamber through a cation exchange membrane (CEM, fumasep FKE, FuMA-Tech GmbH, Germany) fixed with an aluminum cap. Cathode was a high-purity graphite rod ( $\varnothing=0.635$ , 6 cm, C-00-RD-000121, Goodfellow, UK) coated as detailed blow with either In or Sn with a net geometric surface area of 2.5 cm<sup>2</sup>. A rotating disc electrode (RDE) holder (CTV 101T, Tacussel, France) was used in rotating mode for electrochemical pre-treatment steps and without any rotation for eCO<sub>2</sub>RR experiments. Plates of platinized titanium (0.05×1×7 cm, platinode, Umicore Galvanotechnik GmbH, Germany) were used as anodes. Reference electrodes (RE) were Ag/AgCl in saturated KCl (SE 11, +0.197 V vs. SHE, Xylem Analytics Germany Sales GmbH & Co. KG Sensortechnik Meinsberg, Germany) and checked before each experiment. A potentiostat (SP-50, BioLogic Science Instruments, France) was utilized to conduct the pre-treatment and eCO<sub>2</sub>RR experiments in potentiostatic mode. A peristaltic pump (ISMATEC Reglo Analog MS-4/8, Cole-Parmer GmbH, Germany) was used to constantly recirculate anolyte into the anode compartment at a rate of 1.2 mL min<sup>-1</sup>. All of the pre-treatment and eCO<sub>2</sub>RR experiments were performed in an incubator (TH 30, Edmund Bühler GmbH – 72411 Bodelshausen, Germany) at a constant temperature of 30 °C. Components of the electrochemical reactor setup and the steps of eCO<sub>2</sub>RR to formate are illustrated in Figure 1.

eCO<sub>2</sub>RR experiments were conducted for 1 hour at –2.2 V. 50 mM HCO<sub>3</sub> buffer electrolyte solution that resembles low salt conditions was used as a benchmark within the experiments when using a new batch of materials. This enabled us to compare the performance to our previous studies.<sup>[12–14,32]</sup> Composition of MM63 V minimal medium used in high salt eCO<sub>2</sub>RR are provided in Table S1. The pH and conductivity of the modified growth media used throughout the experiments are summarized in Table S2.

### Catalyst electrodeposition

Pre-treatment of the graphite electrodes before electrocatalyst deposition was applied as previously described.<sup>[13,14]</sup> The pre-treatment and electrodeposition were carried out separately before each replicate. For electrodeposition of In, a 50 mL solution of 0.1 M InCl<sub>3</sub> in 1 M acetate buffer (pH 4.5) was used in a single chamber reactor with an applied potential of –0.9 V and a defined charge of 1.7 C. Sn electrodeposition was initially conducted as previously described at electrodeposition potential and charge of –1.0 V and 1 C, respectively.<sup>[37]</sup>

Modified method and process of establishing a procedure for Sn-coated graphite were based on the results discussed in establishment of Sn-electrodeposition part of this study and Supplementary Information. Prior to each eCO<sub>2</sub>RR experiment, the finally prepared electrodes, were washed with deionized water. Further details of the electrocatalyst coating procedures are explained in detail in Supplementary Information.

### Analytical methods

Catholyte samples of 400  $\mu$ L were collected before and after 1-hour eCO<sub>2</sub>RR experiments through the sampling port with a syringe. To detect organic compounds, liquid phase analysis was performed using an HPLC (Shimadzu Scientific Instruments, USA).

Concentration of In and Sn that leached to catholyte was determined with polarograph (797 VA Computrace, Metrohm, Switzerland) equipped with a platinum wire as the counter electrode and an Ag/AgCl in saturated KCl as the reference electrode. Differential pulse (DP) mode was used with a hanging mercury drop electrode (HMDE).<sup>[58]</sup> The external In and Sn standards were calibrated in the range of 0.906 nM to 0.906 mM (four-point calibration, R<sup>2</sup> = 0.99) and 1.08  $\mu$ M to 1.08 mM (four-point calibration, R<sup>2</sup> = 0.99) respectively.

The pH and conductivity were measured with a pH electrode (InLab Micro Pro, Mettler Toledo, Switzerland) and a conductivity probe (InLab 731-ISM, Mettler Toledo, Switzerland) connected to a pH/conductivity benchtop meter (S470, Mettler Toledo, Switzerland).

Gas composition of 1-hour eCO<sub>2</sub>RR experiments were analyzed as previously described.<sup>[12]</sup> Details of the gas phase analysis procedures are explained in detail in Supplementary Information.

### Data processing and calculations

Calculations for coulombic efficiency (CE) and specific rate of formate production ( $r_{\text{formate}}$ ) are described in Supplementary Information.

## Acknowledgements

We thank Philip Haus for experimental advice and technical support for electrochemical reactors. The authors acknowledge the support of the VIVALDI project that has received funding from the European Union's Horizon2020 research and innovation program under grant agreement 101000441. This research is financed by the German Federal Ministry of Education and Research (BMBF) under the GAMES project (Grant nr: 33RC031E). The responsibility for the content lies with the authors. This work was supported by the Helmholtz-Association in the frame of the Integration Platform "Tapping nature's potential for sustainable production and a healthy environment" at the UFZ. Open Access funding enabled and organized by Projekt DEAL.

## Conflict of Interests

The authors declare no conflict of interest.

## Data Availability Statement

The data that support the findings of this study are available from the corresponding author upon reasonable request.

**Keywords:** electrobiorefineries · electrochemical CO<sub>2</sub> reduction reaction · halophilic microorganisms · microbial electrosynthesis · secondary microbial electrochemical technologies

- [1] E. Schuler, M. Morana, P. A. Ermolich, K. Lüschen, A. J. Greer, S. F. R. Taylor, C. Hardacre, N. R. Shiju, G.-J. M. Gruter, *Green Chem.* **2022**, *24*, 8227–8258.
- [2] C. A. Cotton, N. J. Claassens, S. Benito-Vaquerizo, A. Bar-Even, *Curr. Opin. Biotechnol.* **2020**, *62*, 168–180.
- [3] O. Yishai, S. N. Lindner, J. Gonzalez de la Cruz, H. Tenenboim, A. Bar-Even, *Curr. Opin. Chem. Biol.* **2016**, *35*, 1–9.
- [4] A.-P. Zeng, N. J. Claassens, *Eds.* **2022**, *180*, DOI 10.1007/978-3-031-06854-6.
- [5] F. Enzmann, M. Stöckl, M. Pfitzer, D. Holtmann, *Adv. Biochem. Eng./Biotechnol.* **2022**, *180*, 213–241.
- [6] P. Izadi, F. Harnisch, *Joule* **2022**, *6*, 935–940.
- [7] S. Nitopi, E. Bertheussen, S. B. Scott, X. Liu, A. K. Engstfeld, S. Horch, B. Seger, I. E. L. Stephens, K. Chan, C. Hahn, J. K. Nørskov, T. F. Jaramillo, I. Chorkendorff, *Chem. Rev.* **2019**, *119*, 7610–7672.
- [8] J.-P. Jones, G. K. S. Prakash, G. A. Olah, *Isr. J. Chem.* **2014**, *54*, 1451–1466.
- [9] J. Li, M. Zhu, Y. Han, *ChemCatChem* **2021**, *13*, 514–531.
- [10] J. T. Feaster, C. Shi, E. R. Cave, T. Hatsukade, D. N. Abram, K. P. Kuhl, C. Hahn, J. K. Nørskov, T. F. Jaramillo, *ACS Catal.* **2017**, *7*, 4822–4827.
- [11] S. Zhao, S. Li, T. Guo, S. Zhang, J. Wang, Y. Wu, Y. Chen, *Nano-Micro Lett.* **2019**, *11*, 62.
- [12] R. Hegner, K. Neubert, L. F. M. Rosa, F. Harnisch, *ChemElectroChem* **2019**, *6*, 3731–3735.
- [13] R. Hegner, L. F. M. Rosa, F. Harnisch, *Appl. Catal. B* **2018**, *238*, 546–556.
- [14] C. Gimkiewicz, R. Hegner, M. F. Gutensohn, C. Koch, F. Harnisch, *ChemSusChem* **2017**, *10*, 958–967.
- [15] Eur. Comm., [Rep.] 52011PC0025, **2011**.
- [16] X. Hou, Y. Cai, D. Zhang, L. Li, X. Zhang, Z. Zhu, L. Peng, Y. Liu, J. Qiao, *J. Mater. Chem. A* **2019**, *7*, 3197–3205.
- [17] X. Bai, W. Chen, C. Zhao, S. Li, Y. Song, R. Ge, W. Wei, Y. Sun, *Angew. Chem. Int. Ed.* **2017**, *56*, 12219–12223.
- [18] V. S. K. Yadav, Y. Noh, H. Han, W. B. Kim, *Catal. Today* **2018**, *303*, 276–281.
- [19] F. Lei, W. Liu, Y. Sun, J. Xu, K. Liu, L. Liang, T. Yao, B. Pan, S. Wei, Y. Xie, *Nat. Commun.* **2016**, *7*, 12697.
- [20] Y. Zhao, J. Liang, C. Wang, J. Ma, G. G. Wallace, *Adv. Energy Mater.* **2018**, *8*, 1702524.
- [21] L. Jourdin, T. Burdyny, *Trends Biotechnol.* **2021**, *39*, 359–369.
- [22] F. Harnisch, C. Urban, *Angew. Chem. Int. Ed.* **2018**, *57*, 10016–10023.
- [23] H. Li, P. H. Opgenorth, D. G. Wernick, S. Rogers, T. Y. Wu, W. Higashide, P. Malati, Y. X. Huo, K. M. Cho, J. C. Liao, *Science* **2012**, *335*, 1596.
- [24] T. Haas, R. Krause, R. Weber, M. Demler, G. Schmid, *Nat. Catal.* **2018**, *1*, 32–39.
- [25] R. Hegner, K. Neubert, C. Kroner, D. Holtmann, F. Harnisch, *ChemSusChem* **2020**, *13*, 5295–5300.
- [26] M. Stöckl, S. Harms, I. Dinges, S. Dimitrova, D. Holtmann, *ChemSusChem* **2020**, *13*, 4086–4093.
- [27] Y. Tashiro, S. Hirano, M. M. Matson, S. Atsumi, A. Kondo, *Metab. Eng.* **2018**, *47*, 211–218.
- [28] A. PrévotEAU, J. M. Carvajal-Arroyo, R. Ganigué, K. Rabaey, *Curr. Opin. Biotechnol.* **2020**, *62*, 48–57.
- [29] J. Becker, C. Wittmann, *Curr. Opin. Biotechnol.* **2020**, *65*, 118–128.
- [30] M. Liu, H. Liu, M. Shi, M. Jiang, L. Li, Y. Zheng, *Microb. Cell Fact.* **2021**, *20*, 76.
- [31] M. König, J. Vaes, E. Klemm, D. Pant, *iScience* **2019**, *19*, 135–160.
- [32] P. Izadi, A. Kas, P. Haus, F. Harnisch, *Electrochim. Acta* **2023**, *462*, 142733.
- [33] P. I. Larsen, L. K. Sydnæs, B. Landfald, A. R. Strøm, *Arch. Microbiol.* **1987**, *147*, 1–7.
- [34] V. Müller, A. Oren, *Extremophiles* **2003**, *7*, 261–266.
- [35] K. Hobmeier, M. C. Goëss, C. Sehr, S. Schwaminger, S. Berensmeier, A. Kremling, H. J. Kunte, K. Pflüger-Grau, A. Marin-Sanguino, *Front. Microbiol.* **2020**, *11*, 2124.
- [36] S. P. Cummings, D. J. Gilmour, *Microbiology* **1995**, *141*, 1413–1418.
- [37] X. An, S. Li, A. Yoshida, Z. Wang, X. Hao, A. Abudula, G. Guan, *ACS Sustainable Chem. Eng.* **2019**, *7*, 9360–9368.
- [38] K. W. Kimura, R. Casebolt, J. Cimada DaSilva, E. Kauffman, J. Kim, T. A. Dunbar, C. J. Pollock, J. Suntivich, T. Hanrath, *ACS Catal.* **2020**, *10*, 8632–8639.
- [39] K. Hobmeier, M. Cantone, Q. A. Nguyen, K. Pflüger-Grau, A. Kremling, H. J. Kunte, F. Pfeiffer, A. Marin-Sanguino, *Front. Microbiol.* **2022**, *13*, 783.
- [40] A. Nyssölä, J. Kerovuuo, P. Kaukinen, N. von Weymarn, T. Reinikainen, *J. Biol. Chem.* **2000**, *275*, 22196–22201.
- [41] V. Kindzierski, S. Raschke, N. Knabe, F. Siedler, B. Scheffer, K. Pflüger-Grau, F. Pfeiffer, D. Oesterhelt, A. Marin-Sanguino, H.-J. Kunte, *PLoS One* **2017**, *12*, e0168818.
- [42] I. Putu Parwata, D. Wahyuningrum, S. Suhandono, R. Hertadi, *IOP Conf. Ser. Earth Environ. Sci.* **2018**, *209*, 012017.
- [43] D. Zhu, S. Cui, S. Nagata, *Biosci. Biotechnol. Biochem.* **2008**, *72*, 1977–1982.
- [44] D. Sun, Y. Chen, in *Electrochem. Reduct. Carbon Dioxide Fundam. Technol.* **2016**, pp. 103–154.
- [45] Y. Hori, S. Suzuki, *J. Res. Inst. Catal. Hokkaido Univ.* **1983**, *30*, 81–88.
- [46] M. Stöckl, T. Lange, P. Izadi, S. Bolat, N. Teetz, F. Harnisch, D. Holtmann, *Biotechnol. Bioeng.* **2023**, *120*, 1465–1477.
- [47] H. Zhong, K. Fujii, Y. Nakano, *MRS Online Proc. Libr.* **2014**, *1640*, mrsf13-1640-z10–52.
- [48] Q. Zhang, H. Chen, T. Wu, T. Jin, Z. Pan, J. Zheng, Y. Gao, W. Zhuang, *Chem. Sci.* **2017**, *8*, 1429–1435.
- [49] A. Pătru, T. Binninger, B. Pribyl, T. J. Schmidt, *J. Electrochem. Soc.* **2019**, *166*, F34–F43.
- [50] H. K. Lim, H. Shin, W. A. Goddard, Y. J. Hwang, B. K. Min, H. Kim, *J. Am. Chem. Soc.* **2014**, *136*, 11355–11361.
- [51] A. S. Varela, W. Ju, T. Reier, P. Strasser, *ACS Catal.* **2016**, *6*, 2136–2144.
- [52] J. Dolfing, B. Jiang, A. M. Henstra, A. J. M. Stams, C. M. Plugge, *Appl. Environ. Microbiol.* **2008**, *74*, 6126–6131.
- [53] A. Bar-Even, E. Noor, A. Flamholz, R. Milo, *Biochim. Biophys. Acta Bioenerg.* **2013**, *1827*, 1039–1047.
- [54] M. Dunwell, Q. Lu, J. M. Heyes, J. Rosen, J. G. Chen, Y. Yan, F. Jiao, B. Xu, *J. Am. Chem. Soc.* **2017**, *139*, 3774–3783.
- [55] C. W. Lee, N. H. Cho, K. D. Yang, K. T. Nam, *ChemElectroChem* **2017**, *4*, 2130–2136.
- [56] O. Gutiérrez-Sánchez, N. Daems, W. Offermans, Y. Y. Birdja, M. Bulut, D. Pant, T. Breugelmans, *J. CO<sub>2</sub> Util.* **2021**, *48*, 101521.
- [57] Y. Ding, L. Zhang, Q. Gu, I. Spanos, N. Pfänder, K. H. Wu, R. Schlögl, S. Heumann, *ChemSusChem* **2021**, *14*, 2547–2553.
- [58] J. Barek, A. G. Fogg, A. Muck, J. Zima, *Crit. Rev. Anal. Chem.* **2001**, *31*, 291–309.

Manuscript received: July 6, 2023

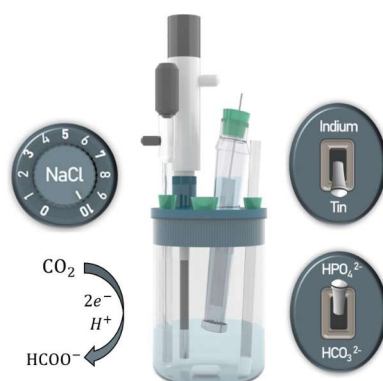
Revised manuscript received: August 7, 2023

Version of record online: ■■■■■



# RESEARCH ARTICLE

**Electrochemical feeding of salt-loving microorganisms:** Halophilic microorganisms are promising for bio-production from formate. Electrochemical  $\text{CO}_2$  reduction to formate necessitates high reaction kinetics, selectivity, and overall efficiency in saline conditions. Starting from a growth media for halophiles adjusting the concentration and composition of salts and buffers in electrolyte solutions enabled higher electrochemical production of formate.



A. Kas, Dr. P. Izadi, Prof. Dr. F. Harnisch\*

1 – 9

**High Salt Electrolyte Solutions Challenge the Electrochemical  $\text{CO}_2$  Reduction Reaction to Formate at Indium and Tin Cathodes**

